

# We are IntechOpen, the world's leading publisher of Open Access books Built by scientists, for scientists

6,900

Open access books available

186,000

International authors and editors

200M

Downloads

Our authors are among the

154

Countries delivered to

TOP 1%

most cited scientists

12.2%

Contributors from top 500 universities



WEB OF SCIENCE™

Selection of our books indexed in the Book Citation Index  
in Web of Science™ Core Collection (BKCI)

Interested in publishing with us?  
Contact [book.department@intechopen.com](mailto:book.department@intechopen.com)

Numbers displayed above are based on latest data collected.  
For more information visit [www.intechopen.com](http://www.intechopen.com)



## Rotary-Die Equal Channel Angular Pressing Method

Akira Watazu  
National Institute of Advanced Industrial Science and Technology (AIST)  
Japan

### 1. Introduction

Light metals such as aluminum, magnesium, titanium and their alloys are useful for a wide range of applications such as in the automotive, railway, and aerospace industries. Engineering of fine-grained light metal materials is an indispensable technology that is expected to improve material properties such as tensile strength, elongation, corrosion resistance, fracture toughness, strain-rate plasticity, low-temperature plasticity, etc. The production of fine-grained light metals with excellent properties using severe plastic deformation methods, especially rolling and extrusion, has been intensively studied. With such processes, the size of the metal grain generally decreases because plastic deformation causes a decrease of grain size, by the principle shown schematically in Fig. 1.

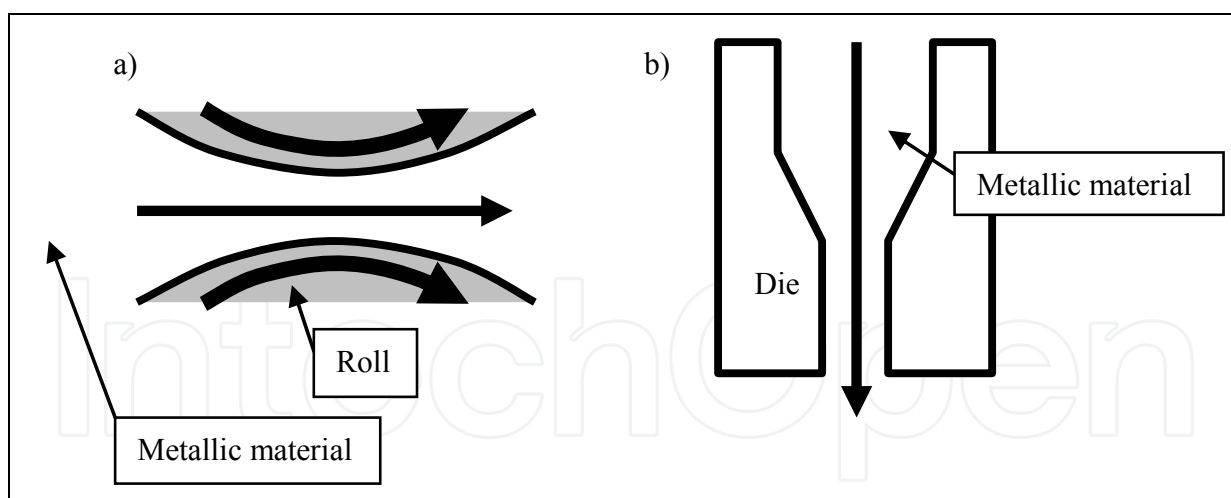


Fig. 1. Schematic diagram of a) rolling method and b) extrusion method

On the other hand, the equal channel angular pressing (ECAP) method invented by Segal et al. in 1981 has proven successful for fabricating fine-grained bulk metals. A schematic diagram of the ECAP method is shown in Fig. 2. In the ECAP method, a large strain can be introduced into a billet sample by simple shear deformation without changes in the cross-sectional area. In the ECAP process, the billet is extruded through a die consisting of two channels intersecting at an angle of  $2\Phi$ . The sample is set in the vertical channel and pressed into the second channel. The greatest advantage of the ECAP method is that the initial size

and shape of the sample processed by the ECAP process are maintained. The sample is enhanced with the shear stress of the angle  $\Phi$  to the extrusion direction in the ECAP process and its structure is fine-grained.

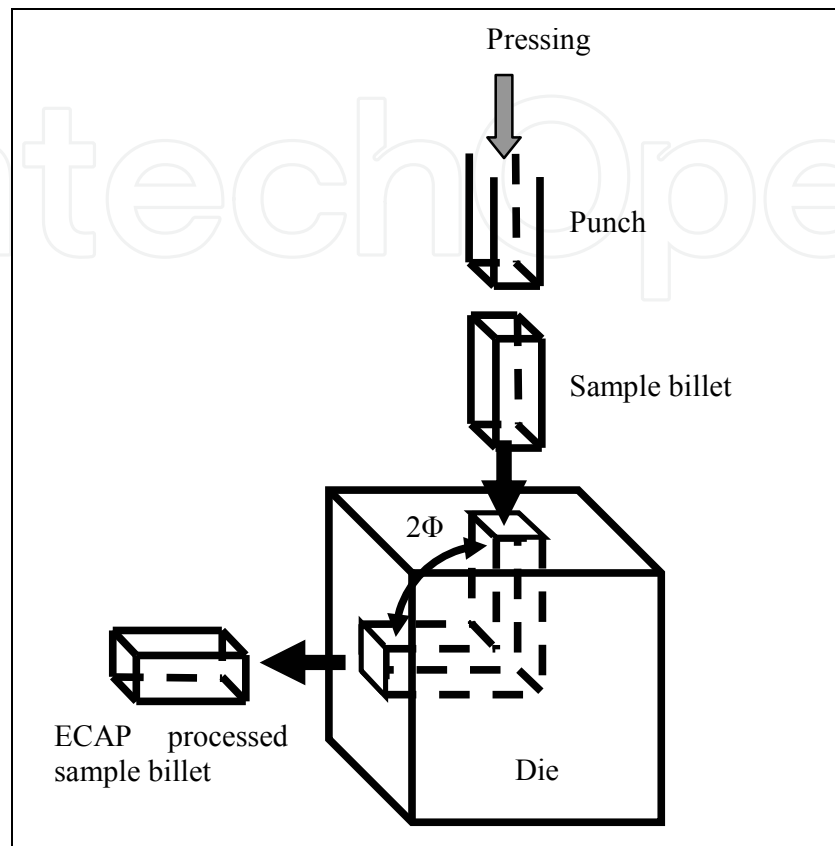


Fig. 2. Schematic diagram of equal channel angular pressing method. (V.M. Segal, V.I. Rexnikov, A.E. Drobysevsky and V.I. Kopylov: *Metally* Vol. 1 (1981), p. 115.)

The rolling method, the extrusion method and the ECAP method are severe plastic deformation methods, and are useful for grain refinement of light metals. In all of these methods, excellent grain refinement is generally expected with many passes. In the case of the rolling method, as shown in Fig. 3-a, the grain is continuously refined with each pass as the material's thickness decreases. In order to process the material with ECAP many times, either a continuous cycling method (Fig. 3-b) or a method of expulsion and reinsertion (Fig. 3-c) are possible. In the case shown in Fig. 3-b, twice or more pressure is necessary when continuing the second time, and there is a limit in the number of ECAP passes depending on the maximum pressure and the die strength. In conventional ECAP, as shown in Fig. 3-c, the pressed sample must be removed from the die and reinserted back for the next pressing, making the process inefficient. Not only does this process take a long time, the temperature of the sample is difficult to control.

A new ECAP process method called the rotary-die equal channel angular pressing (RD-ECAP) method was developed at Japan's National Institute of Advanced Industrial Science and Technology (AIST, formerly the National Industrial Research Institute of Nagoya (NIRIN)) to form fine-grained bulk materials such as aluminum alloys, aluminum composites, magnesium alloys, and titanium. Using the RD-ECAP method, ECAP processing of up to 2 passes can be done without sample removal, and samples processed over 30 cycles were

obtained. One-pass RD-ECAP could be processed in 30 s. In this paper, the RD-ECAP process is explained and its use in the processing of light metals (aluminum alloys) is reported.

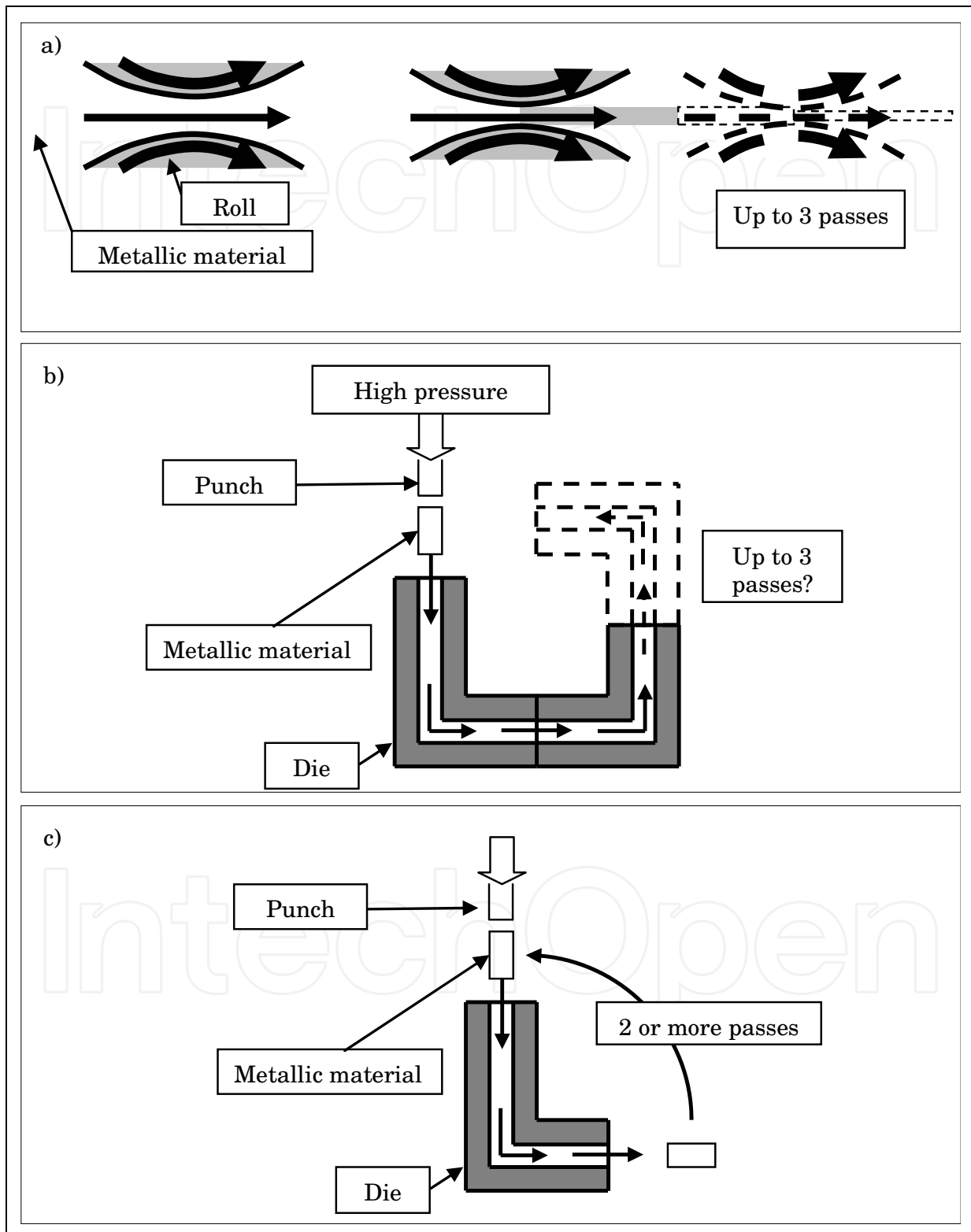


Fig. 3. Schematic diagram of a) rolling method and b, c) the equal channel angular pressing method in the case of two or more passes

## 2. Principle of rotary-die equal channel angular pressing method

The rotary-die equal channel angular pressing (RD-ECAP) method was developed for structuring fine grains in light metal, such as aluminum alloys, magnesium alloys, titanium and so on. In general, using equal channel angular pressing (ECAP), a large strain can be introduced into a billet by simple shear deformation without changes in the cross-sectional area; the billet develops fine grains after several passes of ECAP. However, in conventional ECAP method, the billet must be removed from the die and reinserted back for the next pressing, making the process inefficient. Using the RD-ECAP method, up to 4 passes of ECAP-style severe plastic deformation is possible without billet removal.

Schematic diagrams of the RD-ECAP method are shown in Fig. 4. It consists of four cylindrical channels meeting at the center of the rotary die and four punches in the corresponding channels. The sample is set into the center of the hole. Then, the four punches are placed into the holes from the four directions and the die is set on a die holder. The die is heated to about 500–700 K and a plunger presses the punch at the top. The sample is extruded to the left direction because the right punch and the bottom punch are locked in place due to contact with the die holder. The remaining two channels are used for the conventional ECAP extrusion process. The punch at the top is pushed completely into the die to complete one extrusion or RD-ECAP process. After this extrusion, the die is rotated clockwise 90° to the initial configuration with the exposed punch at the top, and a second pressing is performed. The process continues until the die returns to its former position, after 4 passes. Then, because the sample is not reduced and the die is enough big, temperature of the sample is able to control with control of temperature of the die. The informal name for RD-ECAP is the Japanese term “Mochitsuki”, which is the common process of making rice cake by pressing steamed rice again and again.

In the present work, the samples can be processed under conditions of 573–773K at an approximately 0.9–2.4 mm/s punch speed at 300MPa or lower. By the RD-ECAP method, ECAP processing could be repeatedly done without sample removal. In addition, the temperature of the sample could be easily controlled. In our study, samples processed over 30 cycles (one cycle=one extrusion and 90° die rotation) were obtained. One RD-ECAP cycle could be processed in 30 s. Therefore, RD-ECAP has the advantage of being energy efficient.

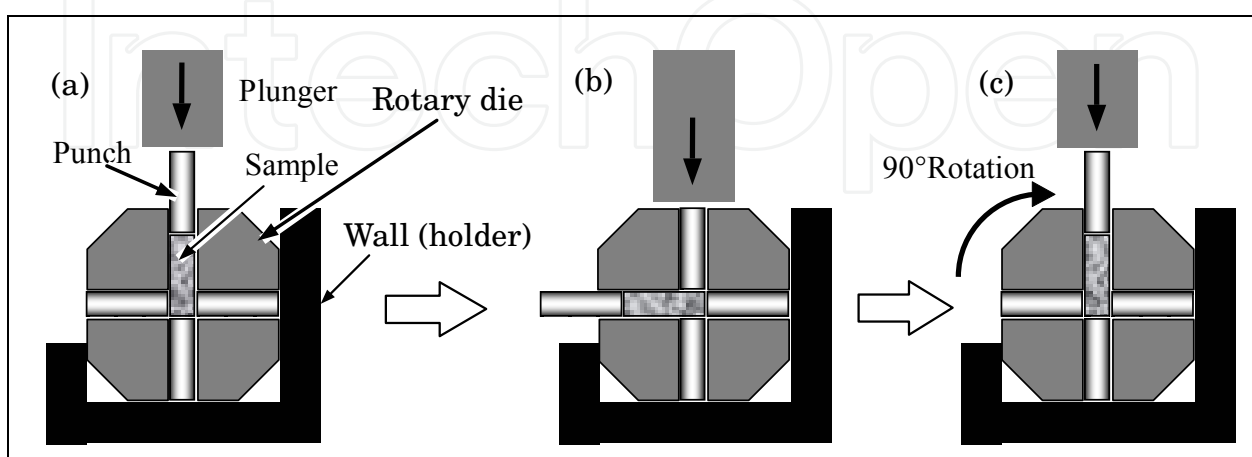


Fig. 4. Schematic diagram of rotary-die equal channel angular pressing. (a) initial state, (b) after one pass, and (c) after 90° die rotation

Compared with the conventional ECAP die consisting of two channels intersecting at an angle, the RD-ECAP die is easy to make because the channels in the RD-ECAP die are formed with two straight holes. Though there are many channels in the RD-ECAP die, the sample is always pressed from the same direction and general press equipment can be used.

### 3. RD-ECAP processed aluminum

#### 3.1 AC4C aluminum alloy

AC4C (JIS, ISO; Al-Si7Mg(Fe)) casting aluminum alloy (Cu<0.20, Si 6.5-7.5, Mg 0.20-0.4, Zn <0.3, Fe<0.5, Mn<0.6, Ni<0.05, Ti<0.20, Pb<0.20, Sn<0.05) is an excellent material for observation of the RD-ECAP effect, such as breaking of the precipitated phase, because the alloy has primary crystal dendrite and a coarse Al-Si microstructure. An AC4C casting aluminum alloy material 20 mm in diameter and 50 mm in length was used. Cylindrical samples 19.5 mm in diameter and 40 mm in length long were prepared by lathing.

The RD-ECAP die had a two cylindrical holes 20 mm in diameter that intersect at 90° to form four channels. Three punches are pushed completely into the side and bottom channels, the sample is placed in the top hole, and the die is set onto a die holder, as shown in Fig. 4-a. Samples were processed under conditions of 543 K, 603K, 673 K at an approximately 0.9 mm/s punch speed from one pass (= one extrusion) to 20 passes.

Photographs of AC4C aluminum alloy samples processed by the RD-ECAP are shown in Fig. 5. The surfaces of the samples were dirty with lubricants but had no cracks or contamination after the RD-ECAP process.

An experimentally obtained load-displacement curve of the plunger for the rotary-die equal channel angular pressing at 603 K is shown in Fig. 6. The load increased with pressing, reached a maximum load, and then decreased with further sample deformation.

Change in the maximum stress with the number of rotary-die equal-channel angular pressing passes is shown in Fig. 7. The maximum load was lower at higher temperatures. At 673K, the first maximum load was about 150 MPa, and the fourth maximum load was about 100 MPa. At 603 K and 543 K, the maximum load decreased as RD-ECAP pass increased from the 1st to 6th pass. The decrease of the maximum load at 603 K was the highest.

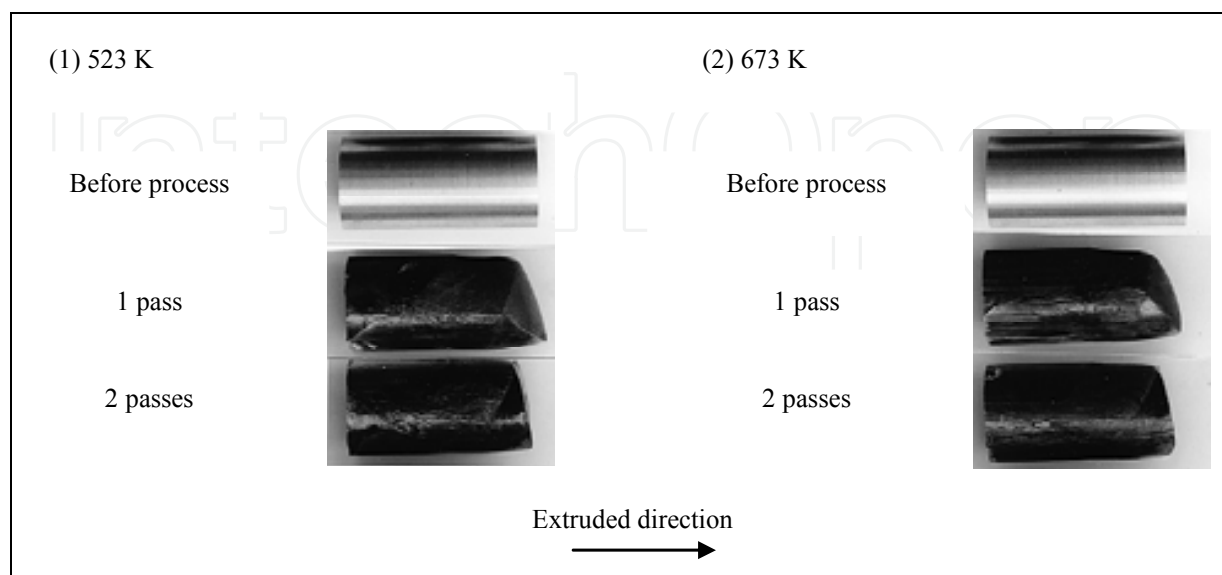


Fig. 5. Photograph of samples processed by rotary-die equal channel angular pressing

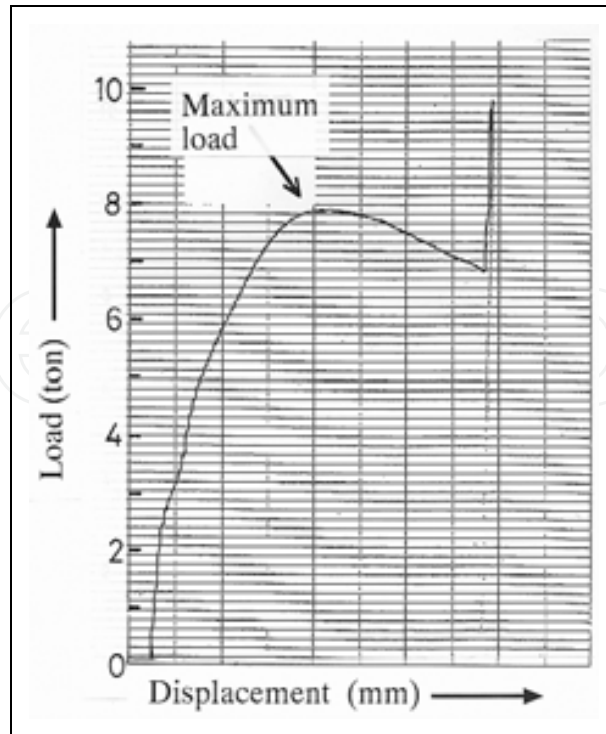


Fig. 6. Experimentally obtained load-displacement curve of the plunger for the rotary-die equal channel angular pressing at 603 K. (Y. Nishida, H. Arima, J.C. Kim and T. Ando: J. Japan Inst. Light Metals. Vol. 50-12 (2000), p. 655-659 in Jp.)

The microstructures of AC4C aluminum alloys processed by RD-ECAP with 1-20 passes at 603 K are shown in Fig. 8. The as-cast sample with 0 passes had a typical aluminium eutectic structure with dendrites. The dendrites were deformed after one pass. After 6 passes, the shape of the primary crystal dendrite disappeared and most eutectic structures were also broken. After 10 passes, the cast structure disappeared. After 20 passes, a uniform microstructure with fine primary-crystal aluminium and fine eutectic structure was observed. The microstructure became fine with increasing of RD-ECAP pass number. In addition, the distribution of the silicon particles appeared to have become more homogeneous with the rising number of RD-ECAP passes.

A TEM photograph of an AC4C aluminium alloy processed by 10 passes of rotary-die equal channel angular pressing at 603 K is shown in Fig. 9. The crystal grains were about 2-3  $\mu\text{m}$ . The relationship between the total elongation and strain rate of the AC4C aluminum alloy processed by the RD-ECAP at 603 K is shown in Fig. 10. The 6-pass sample had about 90 % elongation. The 10- and 20-pass samples had over 100 % elongation, and the maximum elongation was 126 %.

The appearance of the samples after 10-pass RD-ECAP at 603 K and a tensile test at 723 K is shown in Fig. 11. The samples processed by RD-ECAP had smooth surfaces. SEM photographs of the tensile test sample surfaces are shown in Fig. 12. The sample shown in Fig. 12-a had a detailed surface and 111 % elongation. Narrow structure along tensile direction was also shown in Fig. 12-b. By contrast, the as-cast 0-pass sample had many cracks on the 90° direction to the axis of tension and had a rough surface.

By RD-ECAP process, AC4C aluminium alloy hardly had any crack and had the elongation in the tensile test because the microstructure became fine and homogeneous with increasing of RD-ECAP pass number.

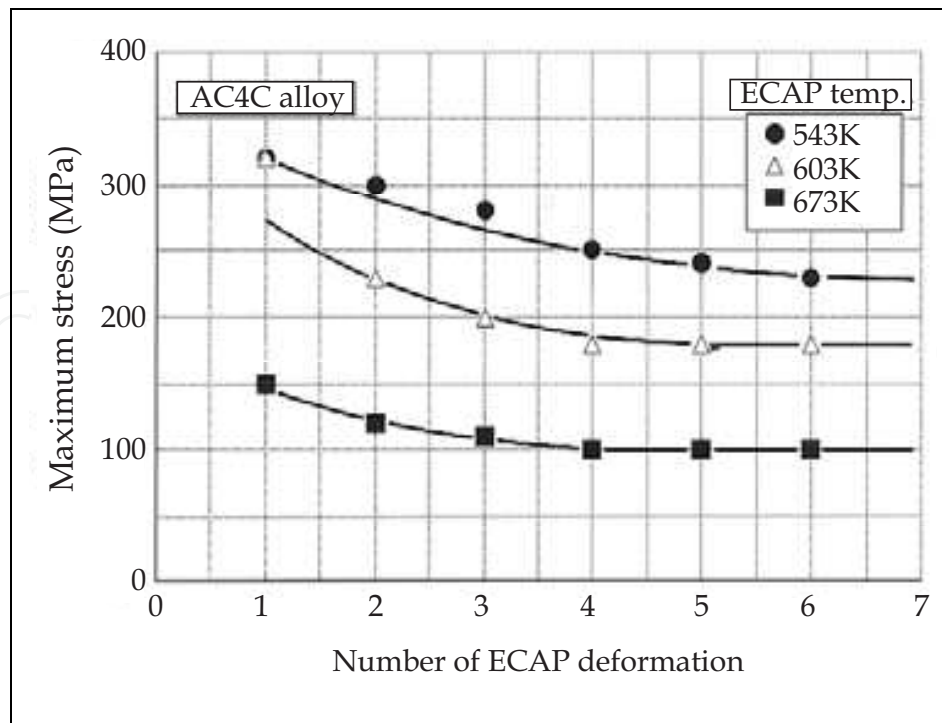


Fig. 7. Change of maximum stress with number of the rotary-die equal channel angular pressing passes. (Y. Nishida, H. Arima, J.C. Kim and T. Ando: J. Japan Inst. Light Metals. Vol. 50-12 (2000), p. 655-659 in Jp.)

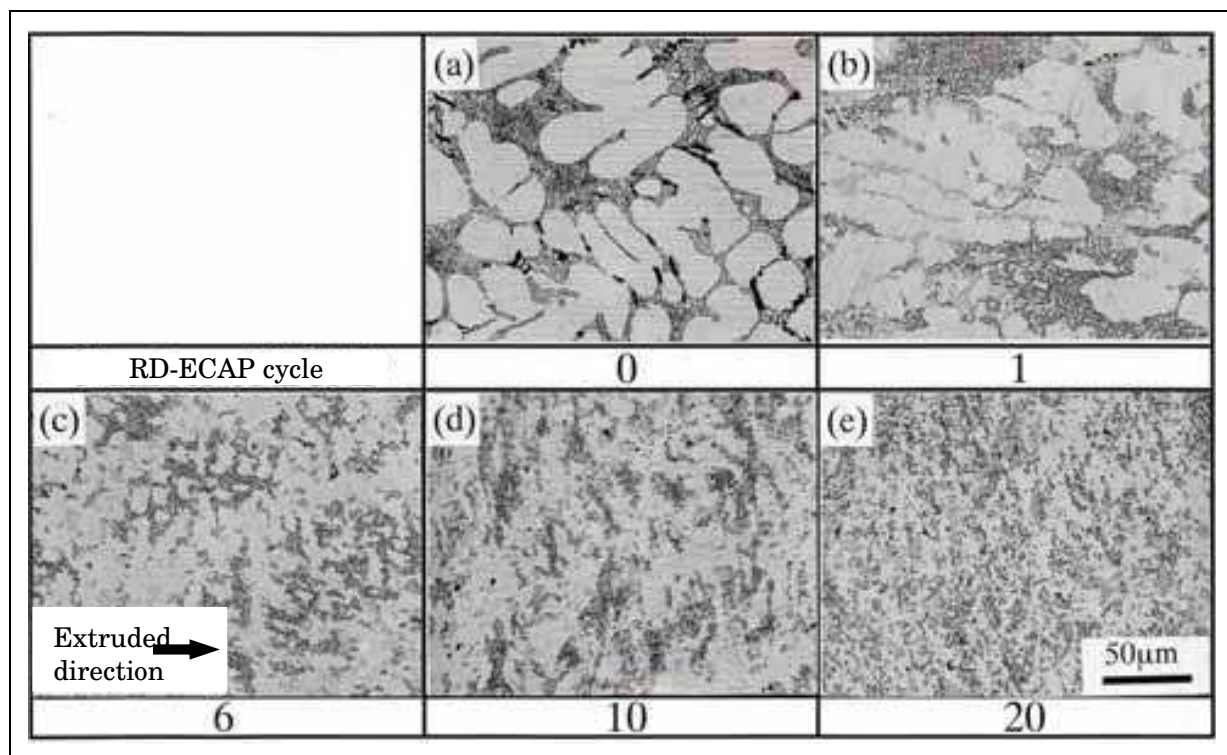


Fig. 8. Microstructures of AC4C aluminum alloys processed by the rotary-die equal channel angular pressing at 603 K. (a) initial state, (b) - (d), after 1-4 passes of RD-ECAP. (Y. Nishida, H. Arima, J.C. Kim and T. Ando: J. Japan Inst. Light Metals. Vol. 50-12 (2000), p. 655-659 in Jp.)

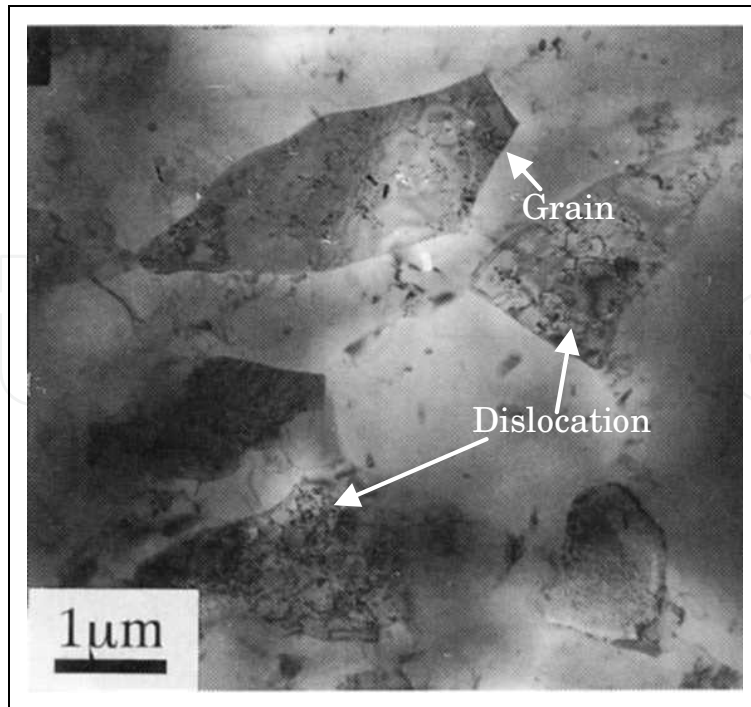


Fig. 9. TEM photograph of AC4C aluminium alloy processed by 10 passes of rotary-die equal channel angular pressing at 603 K. (Y. Nishida, H. Arima, J.C. Kim and T. Ando: J. Japan Inst. Light Metals. Vol. 50-12 (2000), p. 655-659 in Jp.)

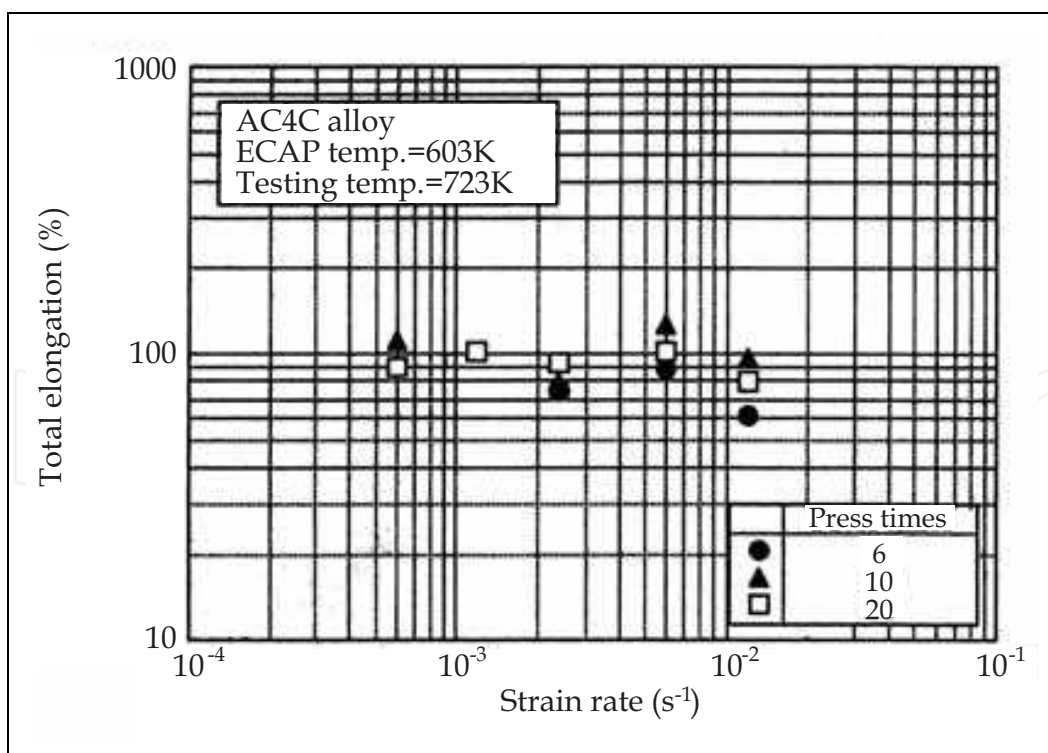


Fig. 10. Relationship between total elongation and strain rate of AC4C aluminium alloy processed by rotary-die equal channel angular pressing at 603 K. (Y. Nishida, H. Arima, J.C. Kim and T. Ando: J. Japan Inst. Light Metals. Vol. 50-12 (2000), p. 655-659 in Jp.)

Strain rate ( $s^{-1}$ )		Elongation (%)
before test		
$5.95 \times 10^{-4}$		111
$2.38 \times 10^{-3}$		79
$5.95 \times 10^{-3}$		126

Fig. 11. Appearance of samples after 10 passes of rotary-die equal channel angular pressing at 603 K and tensile test at 723 K. (Y. Nishida, H. Arima, J.C. Kim and T. Ando: J. Japan Inst. Light Metals. Vol. 50-12 (2000), p. 655-659 in Jp.)

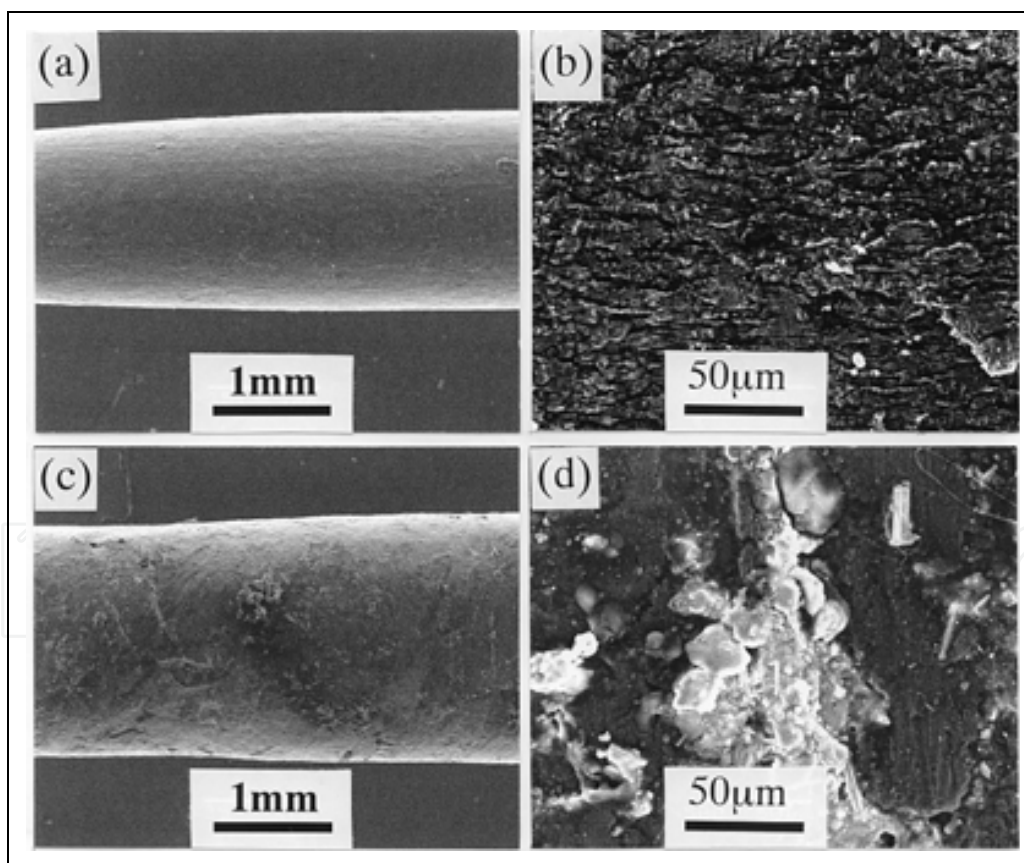


Fig. 12. Tensile test sample surfaces of AC4C alloy observed by SEM after tensile test at 723 K at  $5.95 \times 10^{-4} S^{-1}$ . (a) and (b) are processed by 10 passes of rotary-die equal channel angular pressing at 603 K; (c) and (d) are as-cast samples. (Y. Nishida, H. Arima, J.C. Kim and T. Ando: J. Japan Inst. Light Metals. Vol. 50-12 (2000), p. 655-659 in Jp.)

### 3.2 Al-11mass%Si alloy and impact toughness

Al-Si eutectic alloys are in wide use in industry, especially in the automobile industry, due to their good wear resistance, high tensile strength at elevated temperatures and amenability to casting. However, their low fracture toughness impedes their broader application. Their microstructure consists of eutectic silicon crystals and an aluminum alloy matrix. The silicon crystals, which have three-dimensionally complex shapes and are very brittle, congregate at the grain boundaries of the aluminum matrix. The low fracture toughness of these alloys originates in their microstructure, and is influenced by aluminum dendrite arm spacing and cell size, eutectic silicon characteristics (size and morphology) and eutectic silicon distribution. To improve the microstructure, several techniques are in use industrially: for example, the addition of elements like sodium and strontium. However, this treatment results in little improvement in toughness, since brittleness is thought to be inherent in these alloys.

There are several routes to improving the microstructure of alloys. These include rapid solidification, stirring during solidification, heat treatment, and plastic deformation, with the last being the most energy-efficient.

The Al-11mass%Si eutectic alloy used for the present research contains, by mass, 11.3% Si, 1.00% Cu, 1.13% Mg, 1.10% Ni and 0.277% Fe. The copper, magnesium and nickel are used to improve the mechanical properties of this alloy at elevated temperatures. These elements are present in the alloy as intermetallic compounds including  $Mg_2Si$ ,  $Al_4CuNi$ ,  $Al_9FeNi$ ,  $Al_6Cu_3Ni$  and  $Al_3Ni$ . For RD-ECAP processing, the material of Al-11mass%Si alloy was machined to be a cylindrical billet 19.5 mm in diameter (the channel is 20 mm in diameter) and 40 mm in length. Due to the low billet aspect ratio ( $\approx 2$ ), the billet is subjected to non-uniform deformation, since there is minimal deformation of the billet end zone regions.

The RD-ECAP die had two cylindrical holes 20 mm in diameter that intersect at  $90^\circ$  to form four channels. Three punches are pushed completely into the side and bottom channels, the sample is placed in the top hole, and the die is set onto a die holder, as shown in Fig. 4-a. Then, The die is heated. The effect of RD-ECAP temperature on the impact toughness of the Al-11mass%Si alloy was examined at three temperatures: 573, 623 and 673 K. The billets were processed by RD-ECAP for 4, 8, 12, 16 and 32 passes at each temperature. In addition, four special routes of RD-ECAP were used in this work: (a) 8 passes at 673 K followed by 8 passes at 623 K; (b) 4 passes at 673K followed by 12 passes at 623 K; (c) 4 passes at 573 K followed by 4 passes at 673 K and 8 passes at 623 K; (d) 4 passes at 673 K followed by 4 passes at 623 K and 8 passes at 573 K.

Impact toughness test pieces were made from the RD-ECAP-processed (RD-ECAPed) billet by machining along the longitudinal direction. The size of the rectangular prism test pieces was 3 mm  $\times$  4 mm in cross-section and 34 mm in length, with a U-notch 1.5 mm in width and 1.5 mm in depth. A computer-aided instrumented Charpy impact test machine including software for tougher materials was used for measuring the absorbed energy of the samples as impact toughness during impact testing. The plot in the figure is the average value of four test pieces made from one billet (six pieces in all were made from one billet).

An as-cast alloy was also tested for comparison. An optical microscope and a transmission electron microscope (TEM) were used to observe the microstructures of the RD-ECAPed samples that had been cut from the longitudinal sections of the billets. Proven Solution for Image Analysis was used for investigation of the particle size distribution in the alloy. The maximum diameter of each particle was used as the particle size. A scanning electron microscope (SEM) was employed for observation of the fractured surface.

### 3.2.1 Microstructures

The effect of the number of RD-ECAP passes on the alloy microstructure is shown in Fig. 13, where (a) shows the microstructure of the as-cast alloy, and (b), (c) and (d) illustrate, respectively, the microstructures of samples processed with 8, 16 and 32 passes at 623 K via RD-ECAP. The as-cast (0 pass) sample consists of large grains, including the dendrites of the aluminum matrix, interdendritic networks of eutectic silicon plates and particles of other large intermetallic compounds present between the aluminum dendrite arms or grain boundaries, as shown in this Figure. After pressing by RD-ECAP for 8 passes, the large grains observed in 0 pass sample did not exist and no dendrite structure was found in the alloy. Though  $>20\ \mu\text{m}$  eutectic silicon plates and its interdendritic networks were observed in 0 pass sample, the plates became fine in the samples pressed for multipasses and  $<6\ \mu\text{m}$  plates or particles were observed after pressing by RD-ECAP for 32 passes. In addition, the distribution of the silicon particles appeared to have become more homogeneous with the rising number of RD-ECAP passes. The results indicate that stirring and deformation occurred in the sample by RD-ECAP.

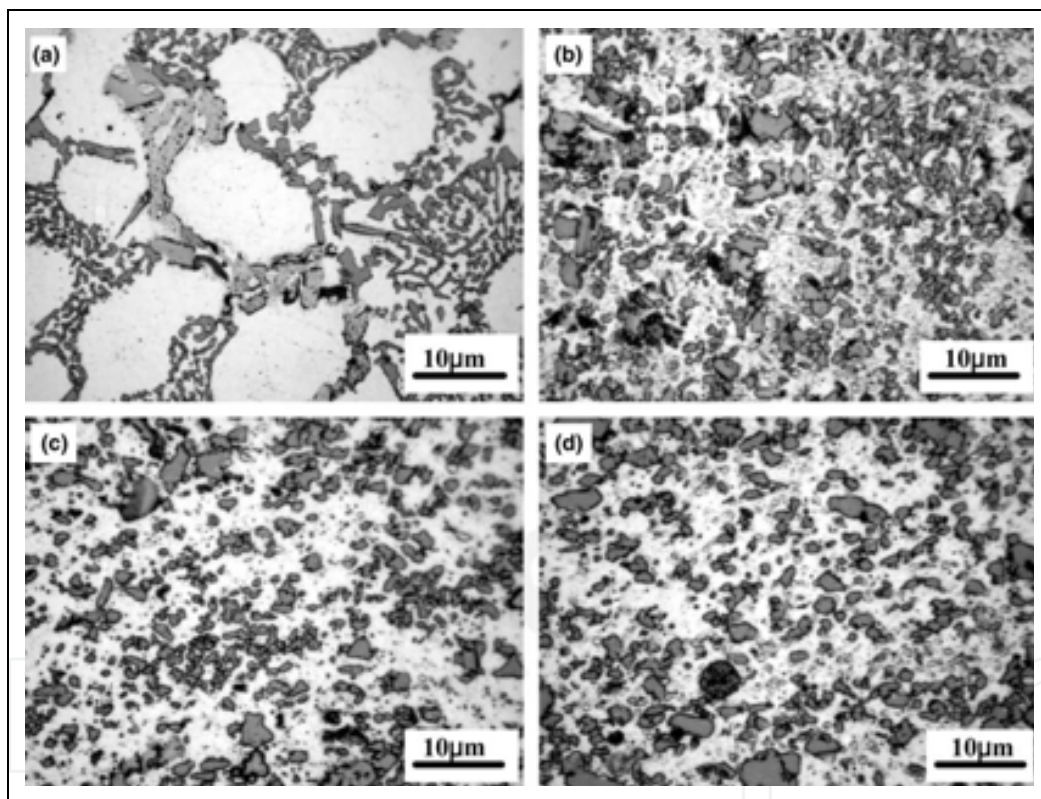


Fig. 13. Microstructures of the Al-11mass%Si samples processed by RD-ECAP at 623 K for (a) – (d) 0, 8, 16 and 32 passes, respectively. (A. Ma, K. Suzuki, Y. Nishida, N. Saito, I. Shigematsu, M. Takagi, H. Iwata, A. Watazu, T. Imura: *Acta Materialia* 53 (2005) 211–220.)

Fig. 14 illustrates the particle size distribution in the alloy after RD-ECAP. Over 60% of the particles are smaller than  $1\ \mu\text{m}$  in the samples processed with 8 and 16 passes at 623 K. After 32 RD-ECAP passes, over 70% of the particles were smaller than  $1\ \mu\text{m}$ . However, the large particle (over  $2\ \mu\text{m}$  in diameter) contents in the samples processed with 8, 16 and 32 passes were not significantly different. It is evident that particles smaller than  $1\ \mu\text{m}$  in the alloy increased with increasing number of RD-ECAP passes.

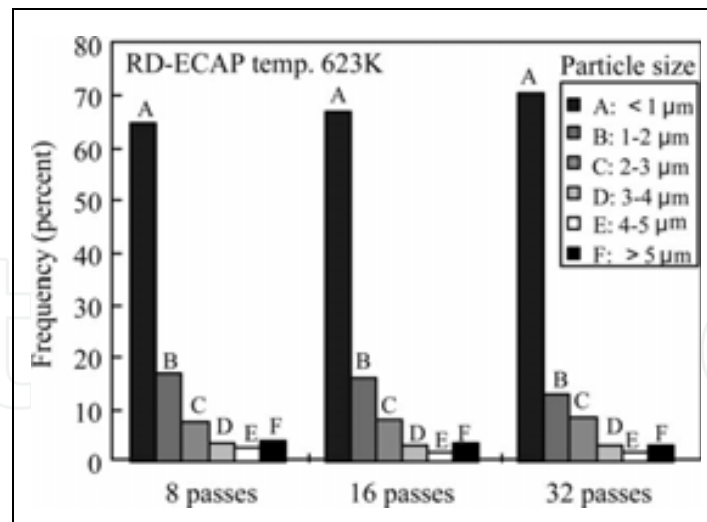


Fig. 14. Effect of the number of RD-ECAP passes on the particle size distribution in the alloy. (A. Ma, K. Suzuki, Y. Nishida, N. Saito, I. Shigematsu, M. Takagi, H. Iwata, A. Watazu, T. Imura: *Acta Materialia* 53 (2005) 211–220.)

Fig. 15 shows the microstructures of the alloy processed with 16 passes by RD-ECAP at three different temperatures: (a) 573 K, (b) 623 K, and (c) 673 K. The particle distribution, including eutectic silicon and intermetallic compounds, seems to have become more homogeneous when the processing temperature increased from 573 to 673 K.

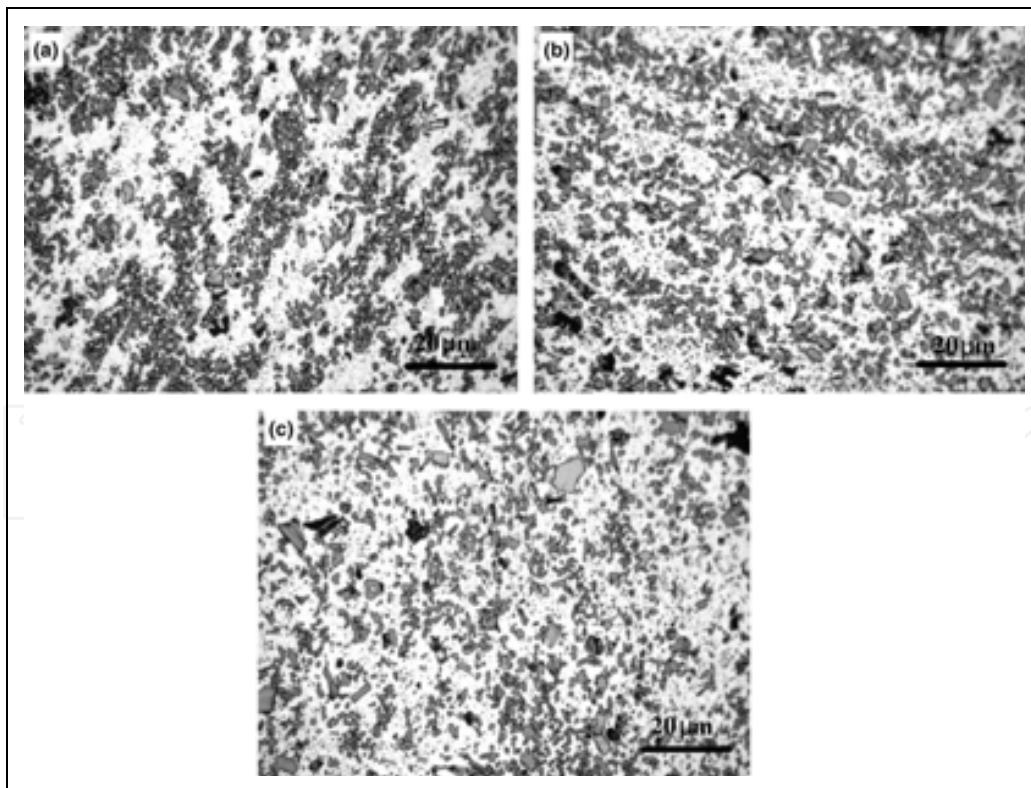


Fig. 15. Microstructures of the Al-11mass%Si alloy processed by RD-ECAP for 16 passes at: (a) 573 K, (b) 623 K, and (c) 673 K. (A. Ma, K. Suzuki, Y. Nishida, N. Saito, I. Shigematsu, M. Takagi, H. Iwata, A. Watazu, T. Imura: *Acta Materialia* 53 (2005) 211–220.)

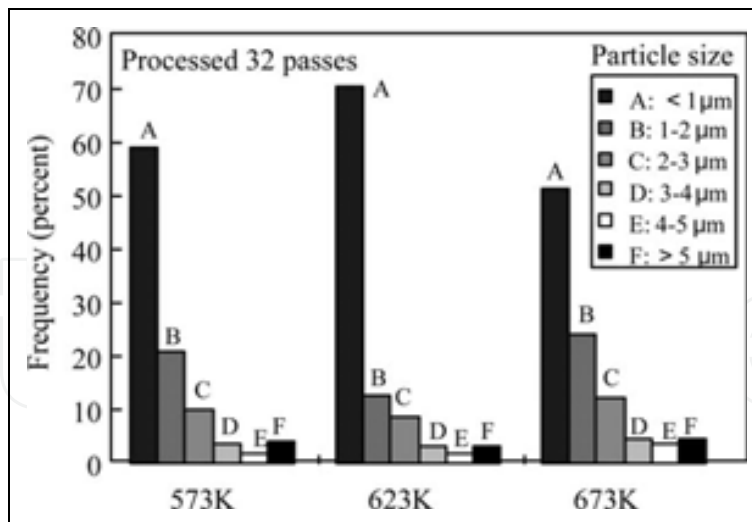


Fig. 16. Effect of the RD-ECAP processing temperature on the particle size distribution in the alloy. (A. Ma, K. Suzuki, Y. Nishida, N. Saito, I. Shigematsu, M. Takagi, H. Iwata, A. Watazu, T. Imura: *Acta Materialia* 53 (2005) 211–220.)

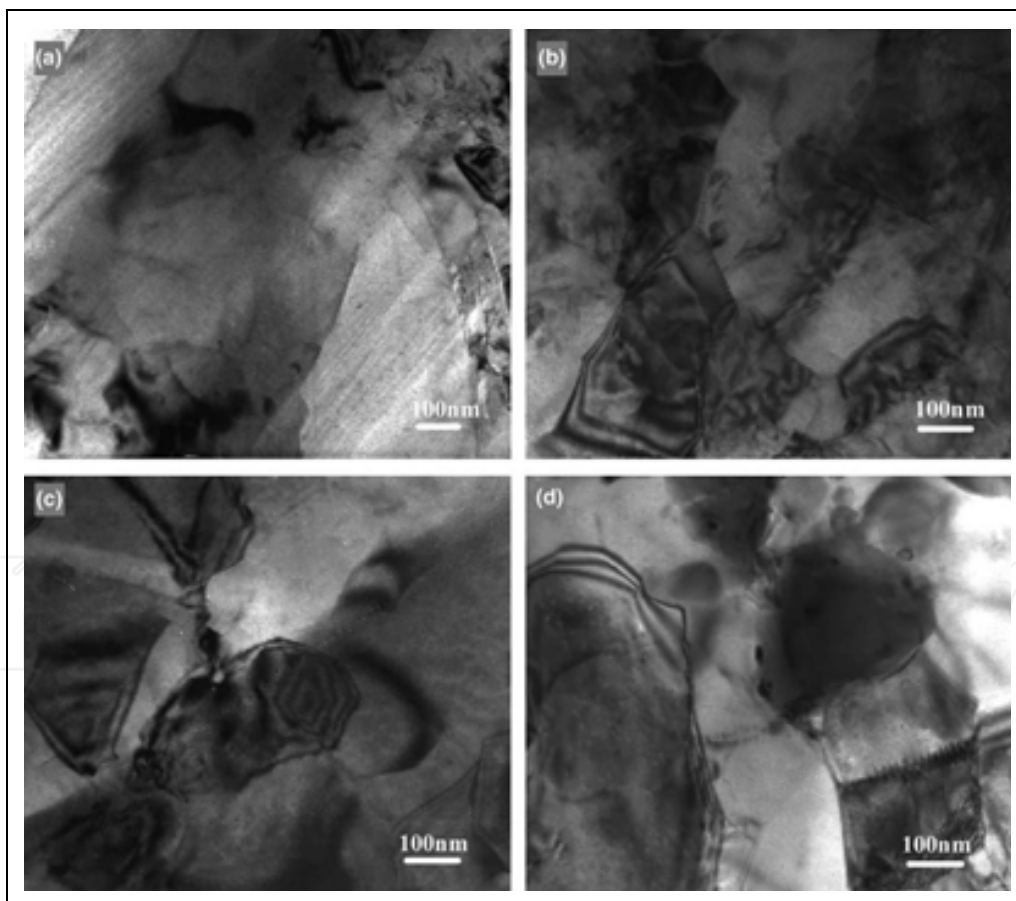


Fig. 17. Transmission electron micrographs of matrix of aluminium in the Al-11mass%Si alloy. (a) as-cast alloy, (b) processed 4 passes, (c) 16 passes, (d) 32 passes by RD-ECAP at 573 K. (A. Ma, K. Suzuki, Y. Nishida, N. Saito, I. Shigematsu, M. Takagi, H. Iwata, A. Watazu, T. Imura: *Acta Materialia* 53 (2005) 211–220.)

Fig. 16 illustrates the particle size distribution after 32 RD-ECAP passes at three different processing temperatures. Among the three samples, the sample processed at 623 K had the highest content of particles smaller than 1  $\mu\text{m}$ . However, no difference in the large particle content ( $> 2 \mu\text{m}$  in diameter) was not clear among the samples processed at the three different temperatures. This result indicates that the processing temperature had little effect on the distribution of large particles.

Fig. 17 shows transmission electron micrographs of aluminum matrix in the Al-11mass%Si alloy, with (a) showing the microstructure of the as-cast alloy, and (b), (c) and (d) showing the microstructures of samples processed by RD-ECAP at 573 K with 4, 16 and 32 passes respectively. It is clear that the grain or grain fragment size of the aluminum was refined after only 4 passes. In spite of the further increase in the number of RD-ECAP passes to 32, the alloy maintained the same grain or grain fragment size of about 200–400 nm.

### 3.2.2 Impact toughness

Fig. 18 shows typical load–displacement curves for the Al-11mass%Si alloy, where curve (a) is the as-cast sample, and (b), (c) and (d) are samples processed by RD-ECAP at 623 K for 4, 16 and 32 passes, respectively. The area below the load–displacement curve of (a) shows the absorbed energy of the as-cast alloy, which is very small in comparison with the results from the other samples.

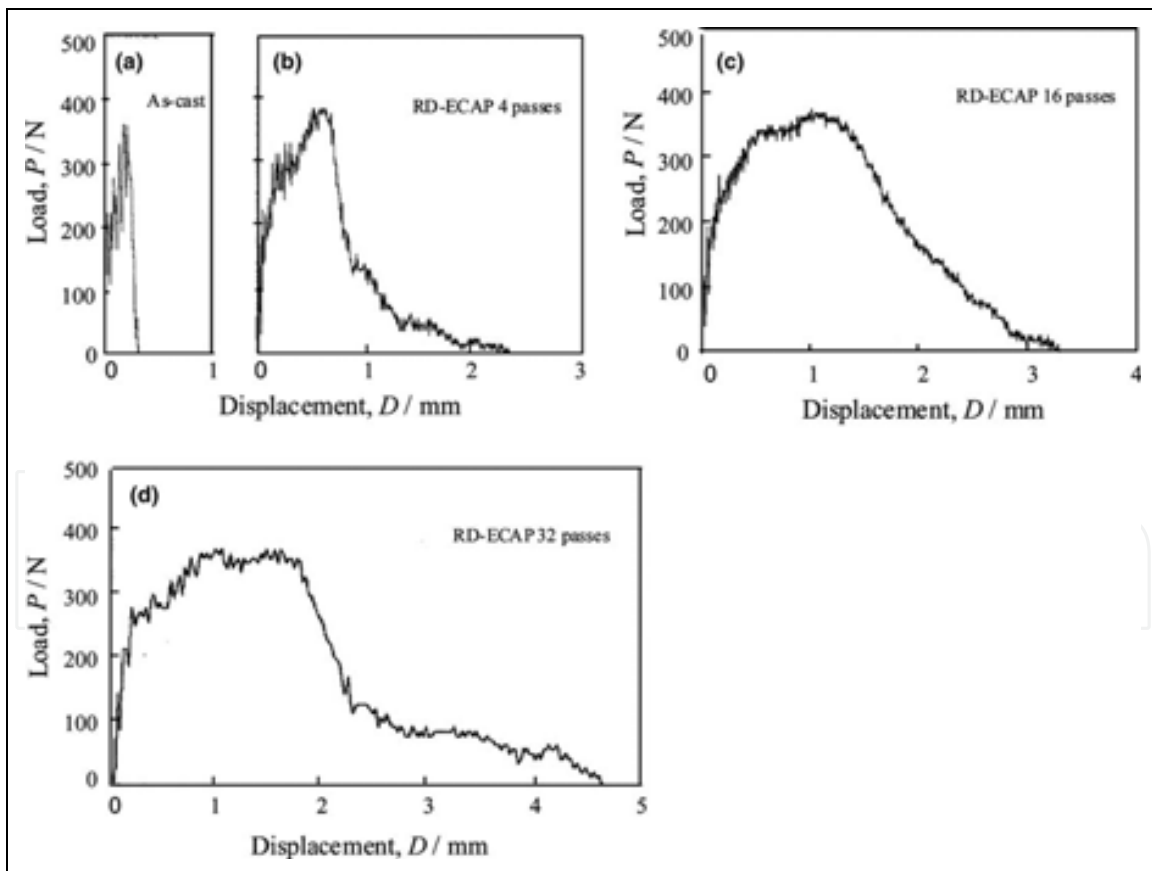


Fig. 18. Typical load–displacement curves of the Al-11mass%Si alloys: (a) as-cast state, (b) (c) and (d) processed by RD-ECAP at 623 K for 4, 16 and 32 passes, respectively. (A. Ma, K. Suzuki, Y. Nishida, N. Saito, I. Shigematsu, M. Takagi, H. Iwata, A. Watazu, T. Imura: *Acta Materialia* 53 (2005) 211–220.)

Fig. 19 shows the relationship between the absorbed energy of the sample during impact testing and the number of RD-ECAP passes. The absorbed energy of the as-cast Al-11mass%Si alloy was 0.9 J/cm<sup>2</sup>. After RD-ECAP, the absorbed energy increased markedly with the increasing number of RD-ECAP passes at all three processing temperatures, ultimately reaching 10 J/cm<sup>2</sup> after 32 passes at 623 K. This value is 10 times that of the as-cast Al-11mass%Si alloy. The relation of RD-ECAP temperature to impact toughness is also shown in Fig. 19, indicating little effect of temperature when the number of RD-ECAP passes is fewer than 12. However, when the number of RD-ECAP passes exceeds 12, a marked effect of RD-ECAP processing temperature on impact toughness is readily observed. This result indicates the existence of a better temperature for RD-ECAP when the number of RD-ECAP passes exceeds 12. For the alloy used in this study, the optimal temperature for RD-ECAP is around 623 K. The effect of the processing route of RD-ECAP on impact toughness is also illustrated in Fig. 19. Using the same number of pressing passes, 16, the additional four routes described in the above section and marked A, B, C and D in Fig. 19 were attempted to achieve high impact toughness. It is evident that the impact toughness of the Al-11mass%Si alloy samples processed by routes A and B were significantly higher than those by other routes; i.e., the samples processed by RD-ECAP for 8 or 4 passes at 673 K followed by 8 or 12 passes at 623 K exhibited relatively high impact toughness.

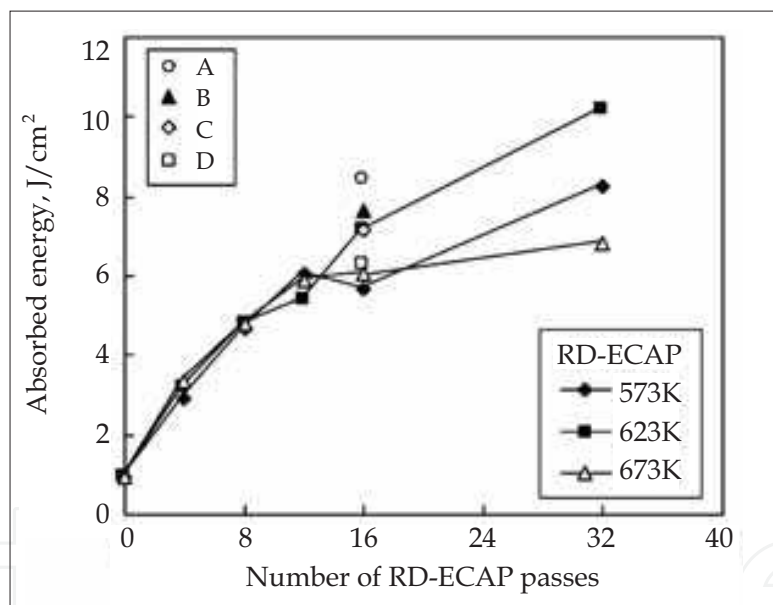


Fig. 19. The absorbed energy of the samples as a function of the number of RD-ECAP passes at 573, 623, 673 K and other routes: (A) at 673 K for 8 passes followed 8 passes at 623 K; (B) at 673 K for 4 passes followed by 12 passes at 623 K; (C) at 573 K for 4 passes followed by 4 passes at 673 K and 8 passes at 623 K; (D) at 673 K for 4 passes followed by 4 passes at 623 K and 8 passes at 573 K. (A. Ma, K. Suzuki, Y. Nishida, N. Saito, I. Shigematsu, M. Takagi, H. Iwata, A. Watazu, T. Imura: *Acta Materialia* 53 (2005) 211–220.)

Fig. 20 shows Charpy impact test pieces without notches after impact tests, in which (a) represents that processed by RDECAP at 623 K for 32 passes and (b) the as-cast alloy. Using the test piece without the notch, the absorbed energy of the sample processed by RD-ECAP at 32 passes could not be obtained because the test piece bent considerably, as shown in Fig. 20(a). However, the test pieces of the unpressed samples fractured in a brittle manner.

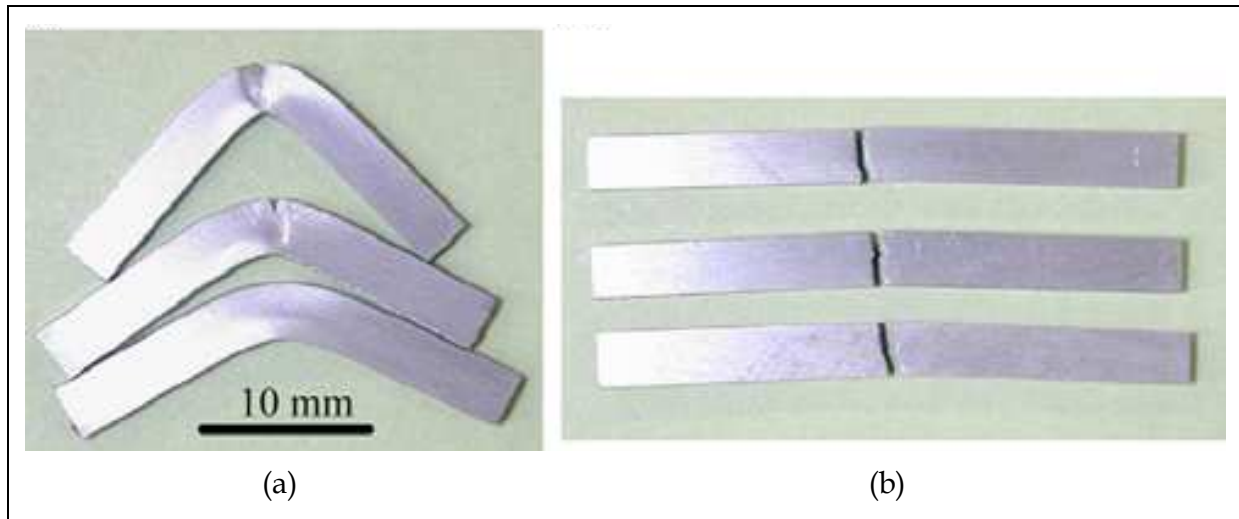


Fig. 20. Impact toughness test pieces without notches of the Al-11mass%Si alloy after testing: (a) processed by RD-ECAP at 623 K for 32 passes; (b) as-cast. (A. Ma, K. Suzuki, Y. Nishida, N. Saito, I. Shigematsu, M. Takagi, H. Iwata, A. Watazu, T. Imura: *Acta Materialia* 53 (2005) 211–220.)

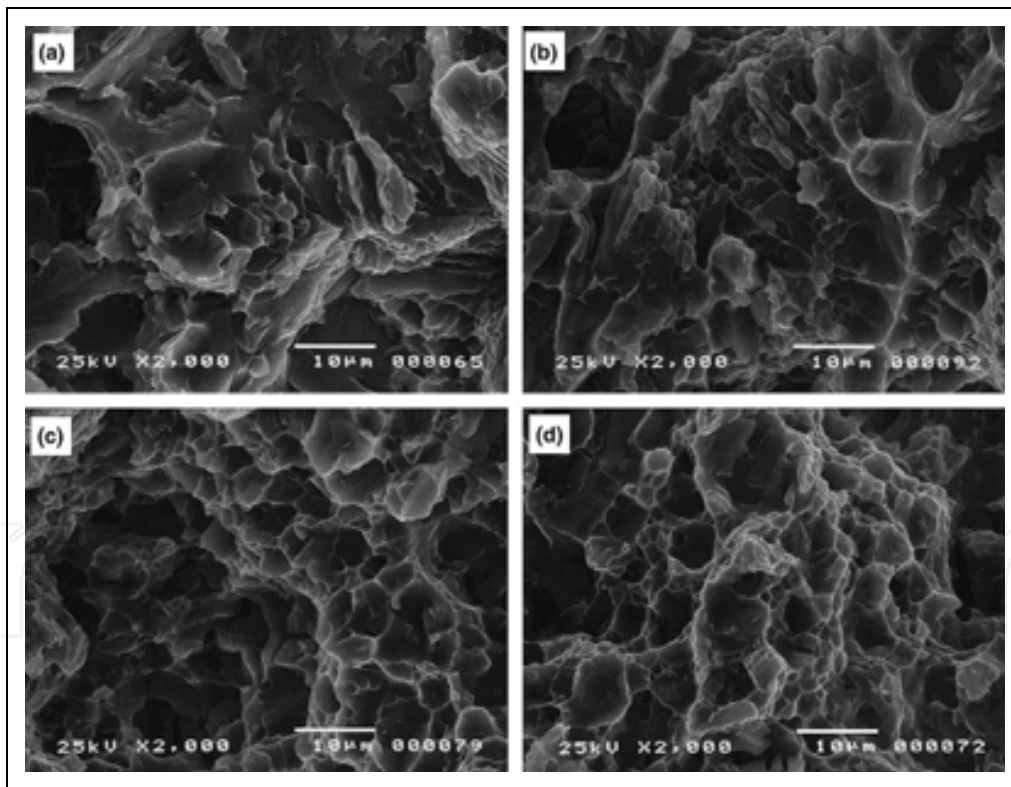


Fig. 21. SEM observations for the fractured surfaces of the Al-11mass%Si alloy: (a) as-cast, (b), (c) and (d) processed by RD-ECAP at 623 K for 4, 16 and 32 passes, respectively. (A. Ma, K. Suzuki, Y. Nishida, N. Saito, I. Shigematsu, M. Takagi, H. Iwata, A. Watazu, T. Imura: *Acta Materialia* 53 (2005) 211–220.)

Fig. 21 shows the fractured surfaces of the test pieces after impact testing, observed by SEM, with (a) representing the as-cast alloy, and (b), (c) and (d) the samples processed by

RD-ECAP at 623 K for 4, 16 and 32 passes, respectively. The as-cast sample shows a rough surface due to the large grains in the alloy and the particles of eutectic silicon and intermetallic compounds at the grain boundaries. The sample processed by RDECAP at 623 K for 4 passes, (b) shows a finer fracture surface, including a couple of dimples, compared to the as-cast sample. The sample RD-ECAPed for 16 passes, (c) shows a fine and homogeneous fracture surface with many dimples. However, little difference can be observed between (c) and (d). A side view of the ductile fracture surface of the Al-11mass%Si alloy processed by RDECAP at 623 K for 32 passes is shown in Fig. 22. The high magnification reveals a typical ductile fracture surface.

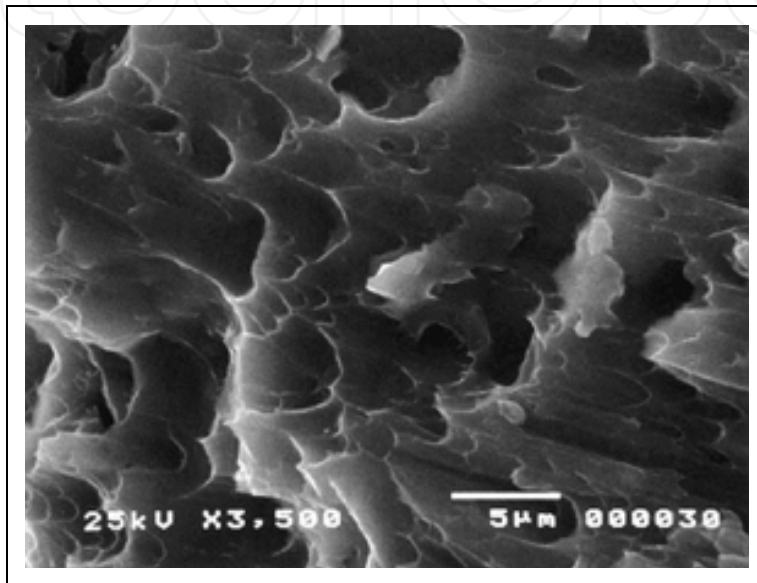


Fig. 22. Side view of a typical ductile fracture surface of the Al-11mass%Si alloy processed by RD-ECAP at 623 K 32 passes. (A. Ma, K. Suzuki, Y. Nishida, N. Saito, I. Shigematsu, M. Takagi, H. Iwata, A. Watazu, T. Imura: *Acta Materialia* 53 (2005) 211–220.)

### 3.2.3 Discussion

As illustrated in Fig. 19, the absorbed energy of the Al-11mass%Si alloy increases with increasing number of RD-ECAP passes. However, after an abrupt increase in the first few passes, generally 4, the increment of absorbed energy gradually levels off with increased RDECAP passes, indicating that the first four passes have the greatest effect on impact toughness. This result is related to the microstructure of the as-cast Al-11mass%Si alloy. As shown in Fig. 13, the microstructure of the as-cast Al-11mass%Si alloy consists of large aluminum grains, including large dendrites and interdendritic networks of eutectic silicon plates, which are the primary reason for the low impact toughness of this alloy. We therefore conclude that breaking up this microstructure and dispersing the eutectic silicon results in improved impact toughness. It appears that the first four RD-ECAP passes do most of the work of breaking the microstructure of the large aluminum dendrites and interdendritic networks of eutectic silicon in the alloy. In fact, during the first 4 RD-ECAP passes, the grain or grain fragment sizes of this alloy are also significantly refined, as shown in Fig. 17(b).

The signal effect of ECAP, as reported in several recent works, is the modification of the grain boundaries. Misorientation angles of grain boundaries are clearly modified during

ECAP. In the present study, RD-ECAP had a similar effect on the grain or grain fragment boundaries. Electron backscatter diffraction (EBSD) can be used to analyze the distribution of misorientation angles ( $\theta$ ) for the aluminum matrix in the RD-ECAPed samples since the grains or grain fragments are very small; i.e., the second particle phase can be ignored. The results for EBSD show that the fraction of high angle boundaries with  $\theta > 15^\circ$  are 65% and 73% for the samples processed by RD-ECAP at 623 K for 8 and 16 passes, respectively. Therefore, the modified grain boundaries produced during RD-ECAP are likely to be an important factor in enhancing impact toughness.

In fact, the experimental results suggest that modified boundaries affect impact toughness. As shown in Figs. 17(b)–(d) and 3, although the diameter of grains or grain fragments did not clearly decrease and the distribution of the larger particles (over 2  $\mu\text{m}$  in diameter) in the sample did not greatly change with increasing the number of RD-ECAP passes, the absorbed energy steadily increased with increased number of RD-ECAP passes, as shown in Figs. 18(b)–(d) and 8. This means that, except for the grain or grain fragment size and the aspect of the particles, other factors such as modified grain or grain fragment boundaries appear to be having an effect during impact testing for improving toughness. We therefore think that if the modified boundaries were eliminated, the impact toughness of this alloy would greatly decrease. To investigate the effect of the modified grain boundaries and the larger silicon particles on the impact toughness, we made two kinds of samples and measured the absorbed energy using Charpy impact tests:

- Sample 1 was processed with 16 passes at 623 K by RD-ECAP, then heat-treated at 793 K for 2 h followed by water quenching (solution treatment).
- Sample 2 was heat-treated under T6 conditions (after solution treatment, aged at 443 K for 10 h) followed by RD-ECAP for 16 passes at 573 K.

Impact testing of sample 1 was carried out immediately after the solution treatment. In this case, the recrystallization of the aluminum alloy would take place during the solution treatment. However, since the precipitation of fine particles before impact testing may have been negligible, the effect of particle precipitation at the boundaries could be ignored. As shown in Fig. 12, large particles, including eutectic silicon and intermetallic compounds, other than the small amounts dissolved in the aluminum matrix during solution treatment, were still evenly distributed in the alloy due to the fact that they were evenly distributed during RD-ECAP. The grain or grain fragment size increased to around 8  $\mu\text{m}$ , meaning the modified grain or grain fragment boundaries were eliminated; however, the average silicon particle size also increased with the disappearance of small particles, compared with Fig. 15(b). Impact testing results show that the absorbed energy of sample 1 fell markedly from 7.2 to 4.0 J/cm<sup>2</sup> after the solution treatment.

As shown in Fig. 13, the large particle size in sample 2 is as large as that in sample 1 but clearly larger than that in the sample shown in Fig. 4(a). However, sample 2 exhibited a higher impact toughness (absorbed energy is 7.1 J/cm<sup>2</sup>) than the sample shown in Fig. 4(a). This result indicates that increased silicon particle size is not the reason for the impact toughness reduction of sample 1. Therefore, three factors are likely to be the chief reasons for the loss of impact toughness after the solution treatment: (a) elimination of the modified boundaries, (b) increased grain or grain fragment size, and (c) disappearance of small particles. On the other hand, although the grain or grain fragment size did not clearly decrease with the increased number of RD-ECAP passes over 4 passes, the impact toughness still markedly increased on increasing the number of RD-ECAP passes from 4 to 32, as shown in Fig. 8. This result means that the incremental value of impact toughness may be

related to grain or grain fragment boundary modification and the increase in the proportion of fine particles (smaller than 1  $\mu\text{m}$ ) because, as stated above, the degree of boundary modification and the fine particle content increased with increased numbers of RD-ECAP passes.

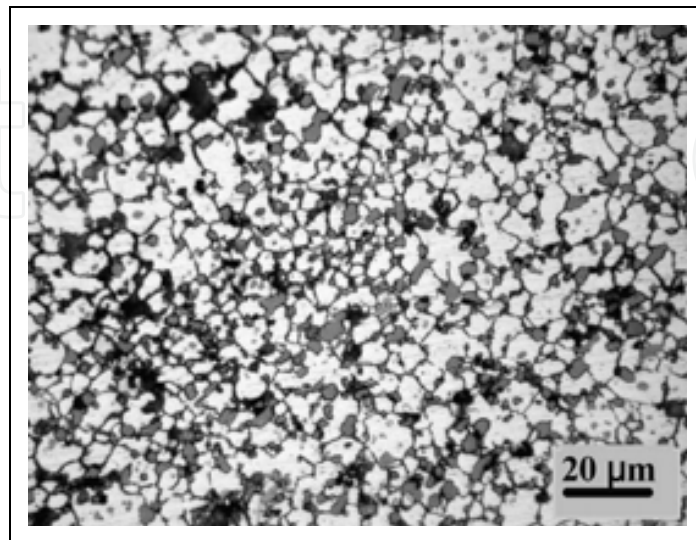


Fig. 23. Microstructure of the Al-11mass%Si alloy processed 16 passes at 623 K by RD-ECAP followed solution treatment at 793 K for 2 h. (A. Ma, K. Suzuki, Y. Nishida, N. Saito, I. Shigematsu, M. Takagi, H. Iwata, A. Watazu, T. Imura: *Acta Materialia* 53 (2005) 211-220.)

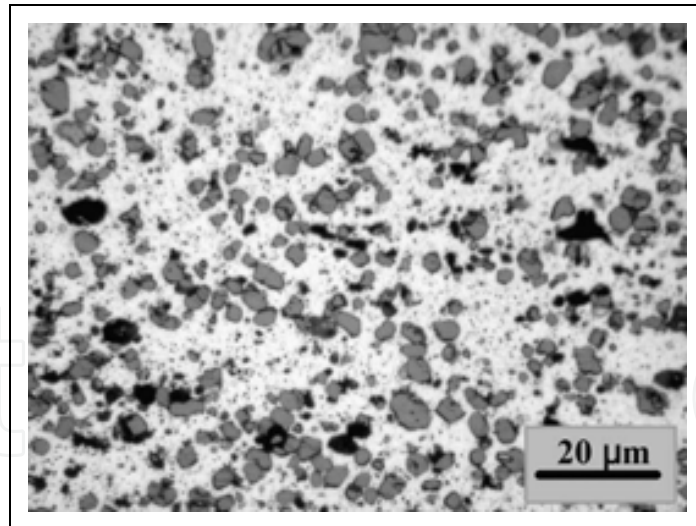


Fig. 24. Microstructure of the Al-11mass%Si alloy heat-treated under T6 conditions (793 K for 2 h then at 443 K for 10 h) followed RD-ECAP at 573 K for 16 passes. (A. Ma, K. Suzuki, Y. Nishida, N. Saito, I. Shigematsu, M. Takagi, H. Iwata, A. Watazu, T. Imura: *Acta Materialia* 53 (2005) 211-220.)

### 3.3 Other aluminum alloy

In the present work, various other aluminum alloys such as Al-23 mass% Si alloy, Si-whisker/extra super duralumin composite, etc., were studied for processing by

RD-ECAP. In the case of Al-23 mass% Si alloy, absorbed energy of a sample processed 32 passes was about 18 times higher than that of a sample processed 0 pass. In the case of Si-whisker/extra super duralumin composite, after pressing by RD-ECAP for 10 passes, grain size was 1.5-2  $\mu\text{m}$  and Si-whisker distribution became homogeneous. Also, Mg alloys and titanium processed by RD-ECAP were studied and the results confirmed that RD-ECAP is useful for forming fine-grained light metal materials.

#### 4. Conclusion

A new ECAP processing method called rotary-die equal channel angular pressing (RD-ECAP) was developed at Japan's National Institute of Advanced Industrial Science and Technology (AIST, formerly the National Industrial Research Institute of Nagoya (NIRIN)), to form fine-grained bulk materials such as aluminum alloys, aluminum composites, magnesium alloy, and titanium. RD-ECAP has the following features:

1. ECAP processing of up to 32 passes (one pass=one extrusion) can be done without sample removal.
2. RD-ECAP saves energy because there is no cooling and re-heating.
3. One-pass RD-ECAP can be processed in 30 s.
4. Over 30 cycles (one cycle=one extrusion and 90° die rotation) of processing were possible in a short time.
5. Aluminium material with fine grain and high impact toughness can be formed.

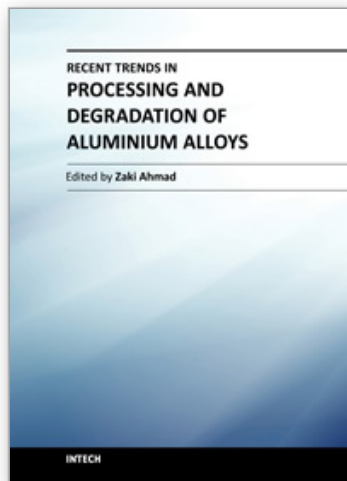
Researches on aluminium processing by ECAP deformation of more than 20 passes are still very few in the world. Therefore, other excellent effects or features are expected to be discovered in the future.

#### 5. Acknowledgment

The author thanks Dr. Yoshinori Nishida and Dr. Aibin Ma for his advice and material offer.

#### 6. References

- Y.H. Zhao, Y.T. Zhu, X.Z. Liao, Z. Horita and T.G.Langdon: *Mater. Sci. Eng.* Vol. A463 (2007), p. 22-26.
- R.Z. Valiev, A.V. Korznikove and R.R. Mulyukov: *Mater. Sci. Eng.* Vol. 168 (1993), p. 141.
- V.M. Segal, V.I. Rensnikov, A.E. Drobysevsky and V.I. Kopylov: *Metally* Vol. 1 (1981), p. 115.
- S.L. Semiatin, V.M. Segal, R.E. Goforth, N.D. Frey and D.P. Delo: *Metall. Mater. Trans. A*, Vol. 30A (1999), p. 1425.
- Y. Nishida, H. Arima, J.C. Kim and T. Ando: *J Japan Inst. Light Metals*. Vol. 50-12 (2000), p. 655-659.in Jp.
- Y. Nishida, H. Arima, J.C. Kim and T. Ando: *J Japan Inst. Metals*. Vol. 64-12 (2000), p. 1224-1229.in Jp.
- A. Ma, K. Suzuki, N. Saito, Y. Nishida, M. Takagi, I. Shigematsu, H. Iwata: *Mater. Sci. Eng. A*, Vol. 399 (2005), p. 181-189.
- A. Ma, K. Suzuki, Y. Nishida, N. Saito, I. Shigematsu, M. Takagi, H. Iwata, A. Watazu, T. Imura: *Acta Materialia* Vol. 53 (2005), p. 211.
- A. Watazu, I. Shigematsu, A. Ma, K. Suzuki, T. Imai, N. Saito: *Mater. Trans.* Vol. 46 (2005), p. 2098.
- A. Watazu, I. Shigematsu, X. Huang, K. Suzuki and N. Saito: *Mater. Sci. Forum* Vol. 544 (2007), p. 419.



## **Recent Trends in Processing and Degradation of Aluminium Alloys**

Edited by Prof. Zaki Ahmad

ISBN 978-953-307-734-5

Hard cover, 516 pages

**Publisher** InTech

**Published online** 21, November, 2011

**Published in print edition** November, 2011

In the recent decade a quantum leap has been made in production of aluminum alloys and new techniques of casting, forming, welding and surface modification have been evolved to improve the structural integrity of aluminum alloys. This book covers the essential need for the industrial and academic communities for update information. It would also be useful for entrepreneurs technocrats and all those interested in the production and the application of aluminum alloys and strategic structures. It would also help the instructors at senior and graduate level to support their text.

### **How to reference**

In order to correctly reference this scholarly work, feel free to copy and paste the following:

Akira Watazu (2011). Rotary-Die Equal Channel Angular Pressing Method, Recent Trends in Processing and Degradation of Aluminium Alloys, Prof. Zaki Ahmad (Ed.), ISBN: 978-953-307-734-5, InTech, Available from: <http://www.intechopen.com/books/recent-trends-in-processing-and-degradation-of-aluminium-alloys/rotary-die-equal-channel-angular-pressing-method>

**INTECH**  
open science | open minds

### **InTech Europe**

University Campus STeP Ri  
Slavka Krautzeka 83/A  
51000 Rijeka, Croatia  
Phone: +385 (51) 770 447  
Fax: +385 (51) 686 166  
[www.intechopen.com](http://www.intechopen.com)

### **InTech China**

Unit 405, Office Block, Hotel Equatorial Shanghai  
No.65, Yan An Road (West), Shanghai, 200040, China  
中国上海市延安西路65号上海国际贵都大饭店办公楼405单元  
Phone: +86-21-62489820  
Fax: +86-21-62489821

© 2011 The Author(s). Licensee IntechOpen. This is an open access article distributed under the terms of the [Creative Commons Attribution 3.0 License](#), which permits unrestricted use, distribution, and reproduction in any medium, provided the original work is properly cited.

IntechOpen

IntechOpen